POLITECNICO DI TORINO
Repository ISTITUZIONALE

A Component Sizing Oriented On-line Controller for Parallel Hybrid Electric Vehicle Powertrains based on the Adaptive Equivalent Consumption Minimization Strategy

Original
A Component Sizing Oriented On-line Controller for Parallel Hybrid Electric Vehicle Powertrains based on the Adaptive Equivalent Consumption Minimization Strategy / Picchirallo, A., Anselma, P.G., Belingardi, G., Emadi, A.. - (2020), pp. 508-513. (2020 IEEE Transportation Electrification Conference & Expo (ITEC) 23-26 June 2020) [10.1109/ITEC48692.2020.9161761].

Availability:
This version is available at: 11583/2843470 since: 2020-09-02T14:08:29Z

Publisher:
IEEE

Published
DOI:10.1109/ITEC48692.2020.9161761

Terms of use:

This article is made available under terms and conditions as specified in the corresponding bibliographic description in the repository

Publisher copyright
IEEE postprint/Author's Accepted Manuscript

©2020 IEEE. Personal use of this material is permitted. Permission from IEEE must be obtained for all other uses, in any current or future media, including reprinting/republishing this material for advertising or promotional purposes, creating new collecting works, for resale or lists, or reuse of any copyrighted component of this work in other works.

(Article begins on next page)

16 September 2026

A Component Sizing Oriented On-line Controller for Parallel Hybrid Electric Vehicle Powertrains based on the Adaptive Equivalent Consumption Minimization Strategy

Alessandro Picchirallo[1,2] , Pier Giuseppe Anselma[1,2] , Giovanni Belingardi[1] , Ali Emadi[2]
[1]Department of Mechanical and Aerospace Engineering (DIMEAS), Politecnico di Torino, Torino, Italy
[2]McMaster Institute for Automotive Research and Technology (MacAUTO), McMaster University, Hamilton, ON, Canada
E-mail: picchirallo.alessandro@gmail.com

***Abstract*-In this paper is illustrated the development of a flexible and near-optimal on-line controller for parallel hybrid electric vehicle (HEV) powertrains based on the well known Adaptive Equivalent Consumption Minimization Strategy (A-ECMS) approach. Guidelines for the developed A-ECMS are automatically extrapolated from a rapid near-optimal off-line HEV controller. Results demonstrate that the implemented version of A-ECMS can remarkably improve the fuel economy performance of the traditional ECMS converging to the off-line near-optimal control benchmark. Moreover, the successful automated application of the developed A-ECMS to two different vehicles sizes suggests its ease of implementation in HEV component sizing processes.**

***Keywords*- Equivalence Factor control , equivalent consumption minimization strategy (ECMS), hybrid electric vehicle (HEV), on-line controller, real-time control.**

I. INTRODUCTION

Component sizing processes for hybrid electric vehicles (HEVs) are usually conducted by maximizing the predicted fuel economy performance according to off-line control approaches [1][2][3]. Off-line HEV controllers optimize the performance of the hybrid powertrain over predefined driving missions by knowing the entire vehicle speed profile before running the simulation. Popular examples include dynamic programming (DP) [4], the Pontryagin's minimum principle [5], the power-weighted efficiency-based rapid control analysis (PEARS) [6] and the slope-weighted energy-based rapid control analysis (SERCA) [7]. However, when developing the on-board real-time HEV controller, achieving the optimal fuel economy performance predicted by the off-line HEV controller might not be guaranteed over all possible driving conditions encountered. To overcome this draft, a recent research trend is emerging in including on-line control already in HEV powertrain design and component sizing processes [8]. Dedicated on-line HEV supervisory control strategies need development in this framework and they should demonstrate simultaneously near-optimal in terms of fuel economy and flexible in being applied to various HEV powertrain arrangements and component sizes [9]. Despite few examples can be found in literature regarding HEV design including on-line control for series [10] and multimode power split layouts [11], little work has been done concerning the implementation of component sizing oriented on-line energy managements strategies (EMS) for parallel HEV powertrains. In order to contribute fulfilling the illustrated research gap, this paper aims at introducing a near-optimal and flexible on-line control approach for parallel HEV powertrains.

The modeling procedure retained here and commonly adopted for vehicle optimization in the early design stages is the quasi-static approach (QSA). QSA considers constant time intervals (usually of 1 second) and works back-ward deriving the value of needed propelling torque from vehicle speed values in adjacent time points [12]. Both computational cost and simulation time can be decreased in this way. The selected HEV layout refers here to a P2 parallel powertrain composed by an internal combustion engine (ICE) and an electric motor generator unit (MGU). In a parallel HEV mechanical power and electrical power can be directly summed up and delivered to the powered axle. Thanks to the high flexibility in its operation the variety of possible arrangements, parallel HEV architectures reveal promising for the automotive industry.

As regards vehicle and chassis data, parameters for two different vehicle sizes will be retained, i.e. a mid-size passenger car and a minivan, while three different transmission configurations will be considered embedding 3, 5 and 8 gears respectively. The possibility of using the developed real-time controller for designing hybrid powertrains for different vehicle sizes and transmission configurations might be suggested in this way.

The proposed on-line HEV controller is based on the combination of two different EMSs from literature. The Adaptive Equivalent Consumption Minimization Strategy (A-ECMS) is particularly retained as on-line control approach, while enhanced and automated calibration of the on-line controller is achieved by means of SERCA as rapid near-optimal off-line HEV control algorithm. The rest of this paper is organized as follows: the parallel P2 HEV architecture is firstly illustrated and modeled. ECMS and SERCA control methods are subsequently recalled, then the development procedure for the proposed component sizing oriented A-ECMS is described. The effectiveness of the proposed HEV control approach is demonstrated by testing its operation on parallel P2 HEV architectures considering two different vehicle types, i.e. a mid-size vehicle and a minivan. Results are finally commented and conclusions are given.

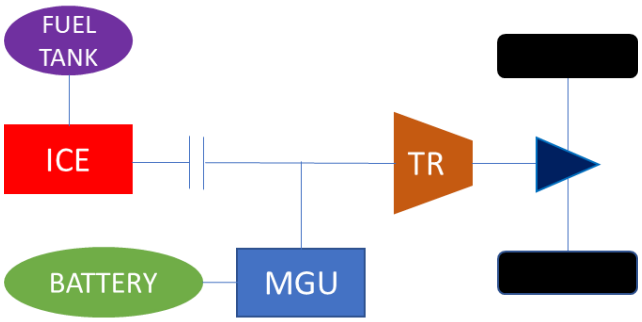

Fig. 1. Parallel P2 HEV Design Scheme.

II. The Parallel HEVs

The two vehicles considered here refer to a mid-size passenger car and a minivan. Vehicle bodies and chassis have been modeled with reference to the coast-down coefficients related to the road load approach [13]. Main parameters for the two considered vehicles and hybrid powertrains are listed in Table 1. The considered parallel P2 HEV is illustrated in Figure 1 and features one ICE and one electric MGU. Values for their mechanical power can be directly summed before entering the transmission (TR). During hybrid operation, both battery charging and regenerative braking can be achieved. Three different transmission configurations have been retained during the calibration involving 3 speed, 5 speed and 8 speed layouts. The gear ratios for the different layouts are reported in Table 2.

The main control actions required for this HEV powertrain architecture are the following [14]:

1. The gear number to be engaged in the gearbox;
2. The ICE status determination (i.e. on/off);
3. In case hybrid operation is selected, the torque split between the ICE and the MGU.

EMSs are needed to control all these features in a HEV powertrain. In the following paragraph, two examples of EMSs will be recalled that lay the foundations for the on-line HEV control approach described in this paper.

TABLE I
Vehicle Data

Data	Unit	**Mid-size**	**Minivan**
Mass	[Kg]	1400	2381
Wheel Radius	[m]	0.301	0.358
RL_A	[N]	100	158
RL_B	[N/m]	3.00	3.25
RL_C	[N/(m/s)^2]	0.15	0.36
ICE Capacity	[l]	1.6	3.6
ICE Max Power	[kW]	65	210
MGU Max Power	[kW]	40	85

TABLE II
Transmission Layouts

Layout	**Gear Ratios**
3 speed	3.50 ; 1.40 ; 0.60
5 speed	3.50 ; 2.00 ; 1.40 ; 1.00 : 0.85
8 speed	4.60 ; 2.72 ; 1.86 ; 1.46 ; 1.23 ; 1.00 ; 0.80 ; 0.68

III. Energy Management Strategies For HEVs

This section aims at reporting the two HEV powertrain control strategies that lay the foundations for the on-line controller developed in this paper. The off-line method used to calibrate the controller is the SERCA algorithm, that consists of three main phases: sub-problems exploration, generalized optimal operating points definitions, energy balance realization [7][15]. The SERCA algorithm has been demonstrated to achieve fuel economy results similar to the DP (that is the most commonly employed HEV off-line control approach) while reducing the corresponding computational cost. In this paper, is adopted the SERCA algorithm as off-line EMS approach to rapidly calibrate the on-line HEV controller and facilitate its implementation in HEV design methodologies.

The proposed sizing oriented on-line HEV controller is based on the ECMS, that is a well known on-line near-optimal EMS and operates by solving at each time instant an optimization problem [16]. The base equation of the equivalent fuel consumption Eq_{FC} to optimize is the following:

$$Eq_{FC} = ICE_{FC} \cdot H_{LHV} + EF \cdot Battery_{Power} \quad (1)$$

The cost function to minimize in this case is characterized by a constant Equivalence Factor (EF) over the retained driving mission between the single costs of fuel power, obtained by the product of the ICE fuel consumption (ICE_{FC}) and the lower heating value of the fuel (H_{LHV}), and battery electrical power ($Battery_{Power}$). The EF usually needs accurate tuning for each HEV powertrain layout and for each drive cycle in order to achieve Charge Sustained (CS) battery operation. The standard ECMS expects to keep the EF as a constant value over the mission. On the other hand, in order to further optimize the controller performance and achieve the CS operation, the A-ECMS modifies the EF over time during the driving mission as illustrated in the following section.

IV. Overview of the Adaptive-ECMS Calibration

In this section, the procedure to develop the proposed component sizing oriented A-ECMS approach will be illustrated. The calibration of the introduced A-ECMS is performed using the SERCA algorithm as a benchmark from which the rules for the on-line HEV EMS are extracted. The workflow of the developed HEV controller is illustrated in Figure 2. Inputs are represented by the velocity (v) and acceleration (a) values for the vehicle for each time step and by an initial supposed value for the EF (EF_0). The torque demand, gear number, and the ICE status are then determined. In case ICE is activated, the torque split needs definition as well. Then, battery state-of-charge (SOC) and overall fuel consumption (FC) can be updated following the QSA as HEV modeling methodology mentioned earlier in this paper.

As detailed later, updating the EF by considering a certain vehicle state variables and proceeding with the following time step will thus be possible. At the end of this procedure, the complete performance of the HEV on the retained drive cycle will be obtained. In the following sub-sections the logic behind each operating step reported in the workflow of Figure 2 is described.

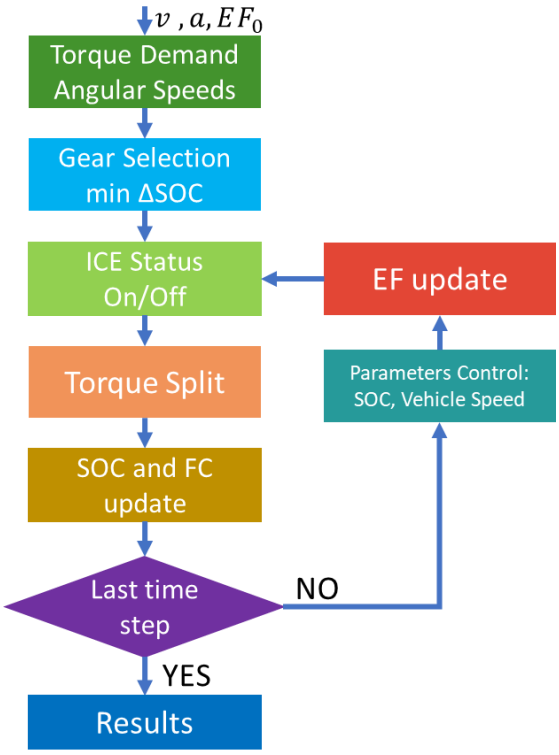

Fig. 2. A-ECMS Workflow.

A. *Torque Demand*

The first step is to calculate the torque demand and the angular speed of the wheels using the road load approach from the velocity and the acceleration of each time step. All the operational parameters related for the ICE, electric MGU and the battery are related to the engaged gear that are presented in the next section.

B. *Gear Selection*

The second step aims at choosing the gear number to engage. For this aim, the gear number engaged over time by SERCA has been analyzed for the mid-size vehicle with a 5 speed trasmission considering 13 common test cycles including WLTP, UDDS, US06 and HWFET as example. A recurrent relationship has been observed between the vehicle speed and the battery power in pure electric mode for the selected gear, as shown in Figure 3. This control action is important to save as much battery energy as possible, considering that SERCA selects pure electric operation for more than 85% of the time associated to the considered driving missions for the retained HEV layout. Following these considerations, in this paper the gear choice corresponds to the minimum variation of the battery SOC, that is linked with the battery power requested by the vehicle in pure electric mode. Another observation rising from Fig. 3 is the dominance of points operated in the highest gear (e.g. the fifth) representing around the 90% of the time instants in which the ICE is not activated. This happens because with equal power required by the motor, a lower rotational speed corresponding to a higher efficiency of the MGU will be achieved. As shown in Fig. 3 the gear selection is not influenced by the EF value. For the on-line control application, operating maps have been created that emulate this gear distribution for the HEV layouts under analysis.

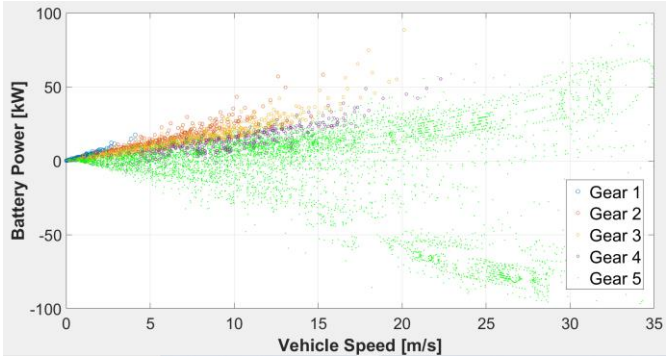

Fig. 3. Gear Distribution in Pure Electric Mode (5 speed mid-size layout).

C. *Ice Status Determination*

The third step of the proposed EMS involves deciding whether to have the ICE operating or not. In this case, SERCA as off-line controller has been observed to reduce both the number of starts and the time spent having the ICE activated. Furthermore, when activated, the ICE is usually employed to charge the battery and achieve CS operation, thus maximizing the effectiveness of the use of fuel energy. Two parameters have been observed being linked with this decision, namely the vehicle power demand, that needs to be positive to allow the ICE operating in acceleration phases, and the battery power, that needs to be negative to charge the battery. Furthermore, reducing the number of ignitions and the time spent in hybrid mode can be possible by observing the ratio between the battery power and the vehicle power demand. A threshold is particularly needed not to activate the ICE too frequently and to use the hybrid mode only when the power requested from the driver is sufficiently high. Keeping the electric mode is therefore suggested during driving conditions that are less aggressive and require less power. In order to select the appropriate mode, the torque threshold changes during the cycle in relation with the SOC and the EF as it will be shown in the following sub-sections. Fig. 4 illustrates the operating mode, i.e. electric or hybrid, selected by SERCA as a function of the electrical power delivered by the battery and the overall vehicle mechanical power demand. Extrapolating a ratio between the two variables illustrated is thus possible to replicate a control behavior similar to SERCA.

D. *Torque Split Determination*

In case the hybrid mode is operated, the next step involves deciding the ratio between electrical and fuel power. In this case, a well-established relationship has been observed between the driver's torque demand and the ICE torque value selected by SERCA. Depending on the size of the engine,

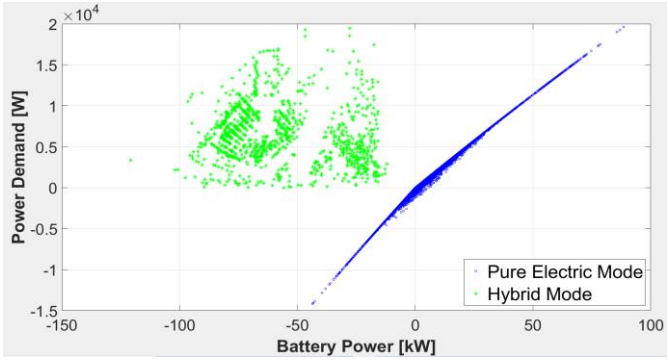

Fig. 4. Pure Electric and Hybrid Modes Distinction (5 speed mid-size layout).

SERCA selects a limited range of ICE torque values during the retained drive cycles, particularly around 80% of the maximum ICE torque. This means that, in order to reduce the FC, it is important to limit the time in which the ICE is activated and to operate it in working points with an high efficiency. In this framework, to be able to rapidly recharge the battery while limiting FC, a right balance between the time spent in hybrid mode and the power produced by the ICE is crucial. Fig. 5 illustrates the relationship between the ratio of ICE torque over total torque demand and the total torque demand as obtained by SERCA in the analyzed driving missions. Fig. 5 is showing how the ICE torque is oscillating in a specific range (e.g. between 75 Nm and 105 Nm, that are the 70% and the 95% of the maximum ICE torque respectively), therefore a fitting curve can be estimated. As shown in Fig. 5, a torque threshold can be set to decide whether the hybrid mode should be operated (e.g. T_{ICE_min}= 90 Nm). In the proposed A-ECMS, the torque split control can be achieved through the EF. Recharging the battery might not be needed in some cases when the battery SOC is high enough. For this reason, the implemented torque threshold is updated at each time instant of the driving mission under analysis depending on the observed value of battery SOC. More details about this procedure are reported in the next section.

E. Equivalence Factor Control

In this paper, a PI controller is employed to control the behaviour of the EF in the proposed A-ECMS as commonly implemented in other versions of this EMS from literature [17][18][19]. The control behaviour of the SERCA algorithm has been analyzed to optimally calibrate the adaptation rules for the EF. Here, calculating the EF is possible at each time step in the following way:

$$\boldsymbol{EF(t)} = -\frac{FC(t)\cdot H_{LHV}}{P_{Batt}(t)\cdot P_{Dem}(t)} \quad (2)$$

To calculate the EF during the mission the instant value of the FC is needed, the battery power (P_{Batt}), the power demand of the vehicle (P_{Dem}), and the low heating value of the fuel (H_{LHV}).

The values of EF operated by SERCA over time has been observed being mainly correlated with vehicle speed and acceleration and with battery power. To develop the EF main control rule, also the range of values of the constant EF that need to be selected for the standard ECMS, to obtain CS operation in different driving cycles for the two vehicles, have been analyzed.

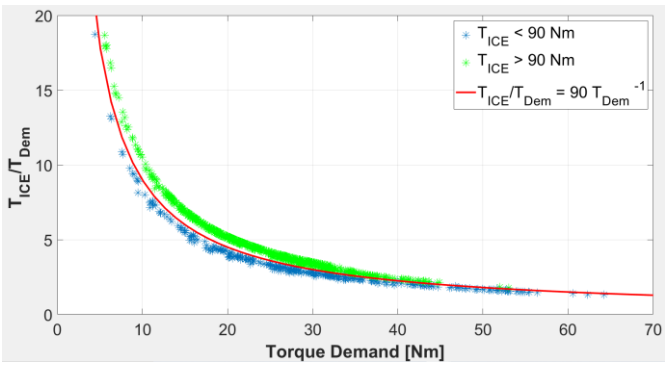

Fig. 5. Torque Split Behaviour (5 speed mid-size layout).

Unlike the traditional non-adaptive ECMS, the initial value of the EF set at the beginning of the driving mission is not crucial. Particularly, the PI controller will adjust the value of EF over time as follows:

$$\boldsymbol{EF(t)} = EF(t-1) + k_p \cdot \big(\Delta SOC(t)\big) + k_t \cdot \int_{t_0}^{t} \big(\Delta SOC(t)\big)\, dt - k_v \cdot \big(v(t) - v(t-1)\big) \quad (3)$$

From this rule we can see that the EF is decreasing with the speed (v) and decreasing with the rising of the SOC level using appropriate coefficients (k_p, k_t, k_v). Some additional constrains are implemented to ensure the CS operation of the HEVs:

a. The battery level can be in the range between the 30% and the 95% of the battery capacity, otherwise the controller will switch mode, starting the ICE or turning it off;
b. The EF can range between 2 and 3, otherwise it incurs in the following penalization:

$$\boldsymbol{EF(t)} = EF(t) + s_{pen} \cdot k_p \cdot [SOC_0 - SOC(t)] \quad (4)$$

With respect to the main control rule (3), a penalization (s_{pen}) is added to keep the EF in the stated range. As mentioned in the previous section, the torque split is influenced by the SOC level to avoid too frequent ICE activations as follows:

$$\boldsymbol{T_{ICE_{min}}(t)} = T_{ICE\,\min_0} - k_T \cdot [SOC_0 - SOC(t)] \quad (5)$$

Here the torque split is tuned by setting a minimum ICE torque (T_{ICE_min}) at each time instant. A coefficient (k_T) can be set starting from a minimum ICE torque (e.g. the 80% of maximum ICE torque) and referring to the starting SOC level (e.g. the 60% of the battery capacity). In case the controller is forced to switch to the hybrid mode, it is necessary to use a flag not to consider the pure electric option and select the best operating point using (1)(3)(4)(5) to calculate EF and T_{ICE_min}. All these features and the parameters can be tuned for a specific vehicle to achieve CS operation in different driving conditions and they can be implemented in an on-line HEV EMS. In order to enhance flexible and automated application of the developed controller to different sizes for vehicle and the powertrain components, a supplementary EF control has been implemented depending on the percentage of the trip covered in length. On one hand this would be possible thanks to recent profuse availability of global positioning systems (GPSs) on passenger cars, on the other hand it would be beneficial for fairly comparing the performance of different component sizes in CS conditions during HEV design processes. The implemented control rules are the following:

a. if the trip % is greater than 75%, the EF and the Torque Split are controlled with a penalization, similarly to (4)(5);
b. if the trip % is greater than 95% , the activation of the ICE will be forced, as described before, in order to achieve the CS operation.

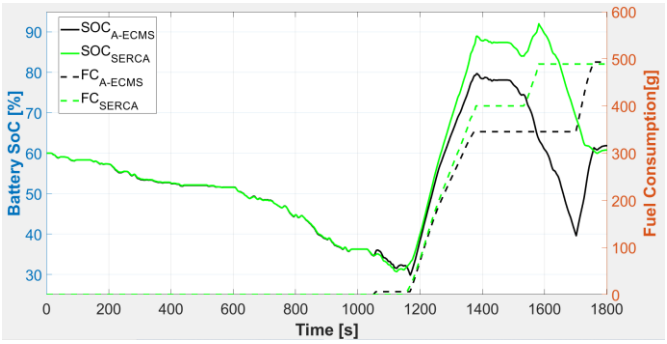

Fig. 6. SOC and FC trend for the 5 speed mid-size layout controlled by SERCA and A-ECMS in WLTP.

V. Results

In this section, simulation results for the developed controller will be shown. A correlation of time histories of vehicle state variables between SERCA and the developed A-ECMS are firstly illustrated. Estimated FC results for different HEV controllers (i.e. SERCA, A-ECMS and traditional non-adaptive ECMS) are then compared over various drive cycles including HWFET, UDDS, US06 and WLTP. In Fig. 6, SOC and cumulated FC values over time are firstly displayed in WLTP for the 5 speed layout of the mid-size vehicle. In the first part of the WLTP cycle in Fig. 6, the SOC trend from A-ECMS overlaps the one from SERCA as a result of the pure electric operation and the appropriate gear selection. Despite the slightly different behavior of SERCA and A-ECMS in the second part of the cycle, both algorithms will end with a very similar FC (489.0 g for SERCA against 493.2 g for A-ECMS), while the final value of SOC for A-ECMS will be close to CS conditions. As regards the EF control, in this example the SOC will reach the 30% needing the A-ECMS controller to activate the ICE to charge the battery. The HEV is operating in the electric mode only for the first 65% of the trip, while the CS operation is reached overall with three ICE starts in order to minimize the FC. These particularly occur after completing the 75% of the trip due to an higher penalization influencing the EF and a lower torque threshold for the ICE activation. Fig. 7 illustrates the corresponding EF trend in WLTP as obtained by the developed A-ECMS. Even the EF fluctuates between 2 and 3 for the most of the time, its overall trend progressively increases until switching to the hybrid mode becomes convenient.

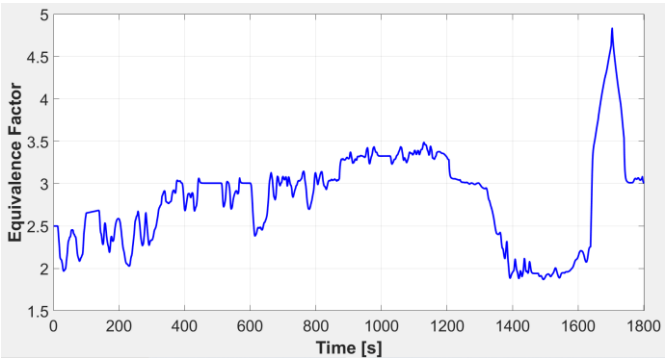

Fig. 7. Equivalence Factor trend for the 5 speed mid-size layout controlled by SERCA and A-ECMS in WLTP.

Focusing on a particular HEV layout, avoiding the use of the trip percentage to penalize more the EF and the torque split might be possible. This could be achieved at the expenses of tuning accurately the parameters in (3)(4)(5). Improving the performance of the controller in terms of FC at the end of the cycle might be possible in this way. This is due to the controller not forcing the activation of the ICE in random points of the mission, but only when convenient, thus reaching the CS operation with a smooth behaviour of the controller. However, as mentioned earlier, flexible application to various HEV component sizes can be achieved by implementing the described EF rule depending on the trip percentage.

TABLE III
Mid-Size 3 Speed Transmission Final Results

Track	FC SERCA [g]	FC A-ECMS [g]	FC ECMS [g]	Difference A-ECMS - SERCA	Difference ECMS – A-ECMS
HWFET	257.15	260.76	361.71	1.40 %	38.71 %
UDDS	142.76	148.12	281.05	3.75 %	89.74 %
US06	220.73	225.19	315.75	2.02 %	40.21 %
WLTP	359.24	364.09	549.46	1.35 %	50.91 %

TABLE IV
Mid-Size 5 Speed Transmission Final Results

Track	FC SERCA [g]	FC A-ECMS [g]	FC ECMS [g]	Difference A-ECMS - SERCA	Difference ECMS – A-ECMS
HWFET	333.96	339.26	481.98	1.59 %	42.07 %
UDDS	179.17	193.91	332.19	8.23 %	71.31 %
US06	250.83	254.37	359.32	1.41 %	41.26 %
WLTP	489.02	493.23	705.19	0.86 %	42.93 %

TABLE V
Mid-Size 8 Speed Transmission Final Results

Track	FC SERCA [g]	FC A-ECMS [g]	FC ECMS [g]	Difference A-ECMS - SERCA	Difference ECMS – A-ECMS
HWFET	287.59	288.69	413.47	0.38 %	43.22 %
UDDS	151.89	168.42	307.09	10.88 %	82.34 %
US06	244.76	247.72	367.19	1.21 %	48.23 %
WLTP	409.80	416.34	600.45	1.60 %	44.22 %

TABLE VI
Minivan 3 Speed Transmission Final Results

Track	FC SERCA [g]	FC A-ECMS [g]	FC ECMS [g]	Difference A-ECMS - SERCA	Difference ECMS – A-ECMS
HWFET	474.24	479.08	582.12	1.02 %	21.51 %
UDDS	243.37	249.25	350.65	2.42%	40.68 %
US06	429.58	431.61	535.24	0.47 %	24.01 %
WLTP	644.16	651.51	852.02	1.14 %	30.78 %

TABLE VII
Minivan 5 Speed Transmission Final Results

Track	FC SERCA [g]	FC A-ECMS [g]	FC ECMS [g]	Difference A-ECMS - SERCA	Difference ECMS – A-ECMS
HWFET	603.40	633.39	700.67	4.97 %	10.62 %
UDDS	303.48	322.14	472.69	6.15 %	46.73 %
US06	580.86	584.52	645.64	0.63 %	10.46 %
WLTP	847.33	849.69	1001.82	0.28 %	17.90 %

TABLE VIII
MINIVAN 8 SPEED TRANSMISSION FINAL RESULTS

Track	FC SERCA [g]	FC A-ECMS [g]	FC ECMS [g]	Difference A-ECMS - SERCA	Difference ECMS – A-ECMS
HWFET	519.75	520.23	547.90	0.09 %	5.32 %
UDDS	248.83	263.97	325.93	6.08 %	23.47 %
US06	498.12	500.90	785.42	0.56 %	56.80 %
WLTP	715.29	718.2	959.70	0.41 %	33.63 %

Finally, a comparison between final values of FC in different cycles for both vehicles is shown in Tables 3-4-5-6-7-8 retaining the three transmission layouts for both vehicle sizes. The proposed A-ECMS is thus demonstrated capable of remarkably improving the ECMS performance in terms of FC (on average by 52.9% and by 23.1% for the mid-size vehicle and the minivan, respectively) while getting closer to the fuel economy performance of SERCA. Overall, UDDS appears the most critical drive cycle as the A-ECMS exhibits a higher FC by 7.6% and 4.9% compared with SERCA for the mid-size and the minivan-type vehicles, respectively. On the other hand, for both HWFET, US06 and WLTP, FC values similar to the ones from SERCA can in general be obtained through the proposed A-ECMS approach. The increase in predicted FC for the A-ECMS is particularly contained within 1.3% and 1.1% on average for the mid-size and the minivan type vehicle, respectively. This can be achieved through the implemented A-ECMS by generating over time control actions comparable to the ones from SERCA both in terms of gear selection, ICE starts and torque split. It can be evinced that the proposed A-ECMS is able to significantly improve the performance of the standard ECMS especially in longer drive cycles (e.g. WLTP or HWFET), by effectively replicating the behavior of SERCA as near-optimal offline controller.

V. CONCLUSIONS

This paper describes the procedure to develop an A-ECMS controller for HEV powertrains using the SERCA algorithm as a calibration tool. The developed real-time HEV controller aims at achieving near-optimality in terms of fuel economy and flexible application to HEV powertrain sizing and optimization processes. All the steps and the rules implemented in the A-ECMS are improving the performances of the controller, thus making its operation comparable with the offline optimized SERCA benchmark. Flexibly tuning the controller parameters has allowed achieving CS operation for different drive cycles considering different vehicle sizes and transmission layouts. Simulation results show how the performance of the developed A-ECMS is close to the one of SERCA in terms of estimated FC while achieving CS battery operation. The FC estimated by the implemented A-ECMS particularly reveals increasing the corresponding value associated with SERCA by only few percentage points in most of the analysed drive cycles. Related future work could aim at showing the potential of the proposed controller in HEV powertrain design processes. Moreover, the behavior of the illustrated A-ECMS controller could be analyzed retaining more detailed HEV models other than the QSA.

ACKNOWLEDGMENT

This research was completed, in part, thanks to funding from the Natural Sciences and Engineering Research Council of Canada (NSERC) and the support of the electrified Powertrain (ePT) team at the McMaster Automotive Resource Centre (MARC) composed by J. Roeleveld, A. Biswas, L. Bruck, A. Lempert, Y. Wang, S. Bonab.

REFERENCES

[1] Y. Yang, K. Aeshad-Ali, J. Roeleveld, and A. Emadi, “State-of-the-art electrified powertrains - hybrid, plug-in, and electric vehicl,” Int. J. Power-trains, Vol. 5, No. 1, 2016.

[2] S. Ebbesen, C. Donitz, and L. Guzzella, "Particle swarm optimization for hybrid electric drive-train sizing,” Int. J. Vehicle Design, Vol. 58, Nos. 2/3/4, 2012.

[3] P.G. Anselma, Y. Huo, J. Roeleveld, A. Emadi, and G. Belingardi, “Rapid Optimal Design of a Multimode Power Split Hybrid Electric Vehicle Transmission,” Proceedings of the Institution of Mechanical Engineers, Part D: Journal of Automobile Engineering, vol. 233, no. 3, pp. 740-762, 2019.

[4] J. Lempert, B. Vadala, K. Arshad-Aliy, J. Roeleveld, and A. Emadi, "Practical Considerations for the Implementation of Dynamic Programming for HEV Powertrains,” 2018 IEEE Transportation Electrification Conference and Expo (ITEC), Long Beach, CA, 2018, pp. 755-760.

[5] A. Chasse, P. Pognant-Gros, and A. Sciarretta, "Online Implementation of an Optimal Supervisory Control for a Parallel Hybrid Powertrain,” SAE Int. J. Engines 2(1):1630-1638, 2009.

[6] P.G. Anselma, Y. Huo, E. Amin, J. Roeleveld, A. Emadi, and G. Belingardi, “Mode-shifting Minimization in a Power Management Strategy for Rapid Component Sizing of Multimode Power-split Hybrid Vehicles,” SAE Technical Paper, 2018-01-1018, 2018.

[7] P.G. Anselma, Y. Huo, J. Roeleveld, G. Belingardi, and A. Emadi, “Slope-weighted Energy-based Rapid Control Analysis for Hybrid Electric Vehicles,” IEEE Transactions on Vehicular Technology, vol. 68, no. 5, pp. 4458 - 4466, 2019.

[8] P. Anselma and G. Belingardi, "Next Generation HEV Powertrain Design Tools: Roadmap and Challenges,” SAE Technical Paper 2019-01-2602, 2019.

[9] P.G. Anselma, Y. Huo, J. Roeleveld, G. Belingardi, and A. Emadi, “From Off-Line to On-Line Control of a Multimode Power Split Hybrid Electric Vehicle Powertrain,” IFAC-PapersOnLine 2019; 52(5): 141-146.

[10] P. Guttenberg, S. Chubbock, and T. Gilbert, "A New Philosophy For Hybrid Vehicle Efficiency Optimisation: Simultaneous Optimisation Of Component Size And Control Strategy For Real-World Efficiency In Hybrid And Electric Vehicles,” SAE Technical Paper, 2011-39-7243, 2011.

[11] P.G. Anselma, Y. Huo, J. Roeleveld, G. Belingardi, and A. Emadi, “Integration of On-line Control in Optimal Design of Multimode Power-split Hybrid Electric Vehicle Powertrains,” IEEE Transactions on Vehicular Technology, vol. 68, no. 4, pp. 3436-3445, 2019.

[12] L. Guzzella and A. Amstutz, "CAE tools for quasi-static modeling and optimization of hybrid powertrains,” in IEEE Transactions on Vehicular Technology, vol. 48, no. 6, pp. 1762-1769, Nov 1999.

[13] H. Karlsson and E. Sörensen, “Road surface influence on rolling resistance: coast-down measurements for a car and an hgv,” Swedish Road Administration, VTI, 2011.

[14] P.G. Anselma, A. Biswas, J. Roeleveld, G. Belingardi, and A. Emadi, “Multi-fidelity near-optimal on-line control of a parallel hybrid electric vehicle powertrain,” 2019 IEEE Transportation Electrification Conference and Expo, Novi, MI, USA, 19-21 June 2019.

[15] P.G. Anselma and G. Belingardi, “Accelerated assessment of optimal fuel economy benchmarks for developing the next generation HEVs,” *20th International Stuttgart Symposium*, Stuttgart, Germany, 17-18 March 2020.

[16] V. Grupta, “Ecms based hybrid algorithm for energy management in parallel hybrid electric vehicles,” Int. J. Technology Innovations and Research, Vol. 14, 2015.

[17] S. Onori, L. Serrao, and G. Rizzoni, “Adaptive equivalent consumption minimization strategy for hybrid electric vehicles,” ASME 2010 Dynamic Systems and Control Conference, DSCC2010-4211, September 12-15, 2010.

[18] A. Rezaei, J. Burl, B. Zhou, and M. Rezaei, “A new real-time optimal energy management strategy for parallel hybrid electric vehicles,” IEEE Transactions on Control Systems Technology, Vol. 27, no. 2, 2019.

[19] F. Zhang, K. Xu, L. Li, and R. Langari, “Comparative study of equivalent factor adjustment algorithm for equivalent consumption minimization strategy for HEVs,” IEEE Vehicle Power and Propulsion Conference, VPPC.2018.8604986, 2018